New Insights into the Functional Behavior of Antibodies as Revealed by Binding Studies on an Anti-Uranium Monoclonal Antibody

Diane A. Blake[1], Xia Li[1], Haini Yu[1], and Robert C. Blake, II[2] [1]Tulane University Health Sciences Center, New Orleans, LA 70112 and [2]Xavier University of Louisiana, New Orleans LA 70125

Abstract

As part of an ongoing effort to develop immunoassays for chelated uranium(VI) on a hand-held flow fluorimeter, an anti-uranium monoclonal antibody designated as 8A11 was fluorescently labeled using two different strategies. When 8A11 was coupled via reactive lysines to either ALEXA™ 488 or Cy5™, the resulting fluorescent antibody conjugate exhibited positive cooperativity in the presence of its antigen, U(VI) chelated with 2,9-dicarboxy-1,10-phenanthroline (U(VI)-DCP). That is, when one of the two binding sites on the covalently modified 8A11 was occupied with bound antigen, the affinity of the remaining site on the antibody for U(VI)-DCP appeared to increase. Unmodified 8A11 bound U(VI)-DCP with the expected hyperbolic dependence on the concentration of antigen, consistent with independent and equal binding of ligand at both sites. Proteolytic cleavage of the fluorescently conjugated 8A11 to produce the fluorescent monovalent Fab fragment yielded an active preparation that now bound U(VI)-DCP with no evidence of positive cooperativity. Although, in principle, any divalent antibody has the potential to exhibit positive cooperativity in its binding interactions with its antigen, very little literature precedent for this type of behavior exists.

Native 8A11 was also noncovalently labeled with highly fluorescent ZENON™ reagents. These reagents are fluorescently-labeled Fab fragments of goat anti-mouse antibodies that bind to the Fc portion of 8A11. These high-affinity, monovalent fluorescent reagents permitted the intact 8A11 mouse antibody to be labeled in situ with no covalent modifications. Incubation of the 8A11 with ZENON 647 produced a fluorescent protein complex that showed an 8-fold higher affinity for U(VI)-DCP than did the free 8A11 alone. Again, very few literature precedents exist for this phenomenon, where agents that bind to the Fc portion of an intact antibody change the affinity of the antibody for the antigen at the structurally distant Fab portion of the molecule.

The addition of protein G, a bacterial protein that also binds to the Fc portion of mouse IgG, to the covalently modified 8A11 produced an antibody preparation that showed a lower affinity for U(VI)-DCP than that observed in the absence of protein G. This protein G-dependent decrease in the affinity of 8A11 for U(VI)-DCP was dose-dependent. Similarly, U(VI)-DCP was observed to decrease the affinity between 8A11 and protein G, also in a dose-dependent matter. These reciprocal binding effects between protein G and U(VI)-DCP were taken as further evidence that binding to the Fc portion on the intact 8A11 antibody could influence the strength of the interaction at the antigen binding sites on the Fab portions of the protein, and vice versa.

These practical, development-driven binding experiments have revealed a fundamental facet of antibody functional behavior that appears to have been largely unnoticed. The binding phenomena described for the first time in this report may have physiological relevance and can be purposefully exploited to improve the sensitivity and utility of selected immunoassays.

Table 1. Equilibrium dissociation constants for the binding of selected phenanthroline derivatives in the presence and absence of uranyl ion to monoclonal antibodies 12F6, 10A3, and 8A11.

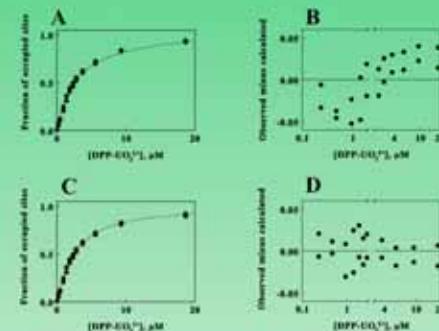| Chelator Complex	12F6	10A3	8A11
DCP-UO$_2^{2+}$	$9.1 \pm 0.7 \times 10^{-10}$	$2.4 \pm 0.2 \times 10^{-8}$	$5.5 \pm 0.2 \times 10^{-8}$
DME-UO$_2^{2+}$	$2.5 \pm 0.1 \times 10^{-8}$	$7.6 \pm 0.2 \times 10^{-8}$	$1.2 \pm 0.1 \times 10^{-6}$
DHM-UO$_2^{2+}$	$7.5 \pm 0.4 \times 10^{-9}$	$3.3 \pm 0.1 \times 10^{-7}$	$8.6 \pm 0.3 \times 10^{-6}$
DPP-UO$_2^{2+}$	$4.5 \pm 0.3 \times 10^{-8}$	$6.3 \pm 0.2 \times 10^{-7}$	$8.7 \pm 0.6 \times 10^{-6}$
DCP, metal free	$7.5 \pm 0.5 \times 10^{-7}$	$2.8 \pm 0.1 \times 10^{-6}$	$3.7 \pm 0.2 \times 10^{-6}$
DME, metal free	$8.7 \pm 0.6 \times 10^{-7}$	$3.4 \pm 0.3 \times 10^{-6}$	$4.4 \pm 0.2 \times 10^{-6}$
DHM, metal free	$1.8 \pm 0.2 \times 10^{-6}$	$5.1 \pm 0.4 \times 10^{-6}$	$6.7 \pm 0.3 \times 10^{-6}$

Figure 1. Assay to distinguish between homogeneous and synergistic binding of chelated uranium to monoclonal antibody 8A11. A, equilibrium binding of the DPP-UO$_2^{2+}$ complex to 8A11 covalently modified with Alexa 488. The curve drawn through the data points was generated from the one-site, homogeneous binding model using a value for K0.5 of 2.93 μM. B, residual plot showing the differences among the experimental data from A and theoretical data calculated using the one-site homogeneous model. C, same binding data as A; the curve was generated from the multiple-site, synergistic binding model represented by the Hill equation, using values for K0.5 and the Hill coefficient of 2.52 μM and 1.17, respectively. D, residual plot showing the differences among the experimental data from A and theoretical data calculated using the Hill Equation.
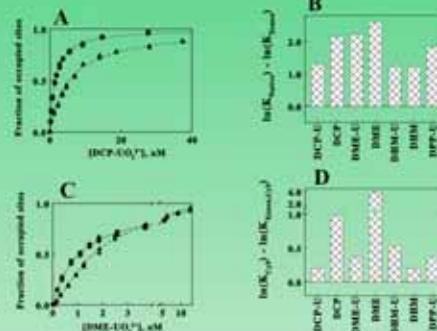

Figure 2. Equilibrium binding of chelators and chelated uranium to covalently modified 8A11. A, binding of DCP-UO$_2^{2+}$ to 8A11 covalently modified with Alexa 488. The solid curve drawn through the data points was generated using the Hill Equation and values for K0.5 and the Hill coefficient of 6.26 nM and 1.60, respectively. The dashed curve represents the binding curve for the one-site, homogeneous binding of DCP-UO$_2^{2+}$ to native, unmodified 8A11 as determined previously. B, values of the Hill coefficients obtained from the binding curves of four different chelator-uranium complexes to 8A11 covalently modified with either Alexa 488 (solid pattern) or Cy5 (diagonal pattern). C, differences in the natural logarithms of the values for K0.5 obtained previously for the binding of seven same compounds to 8A11 covalently modified with Alexa 488. D, differences in the natural logarithms of the values for K0.5 obtained for the binding of seven antigen analogs to native 8A11 minus those obtained for the binding of the same compounds to 8A11 covalently modified with Cy5.

Figure 4. Equilibrium binding of chelators and chelated uranium to 8A11 noncovalently modified with Zenon 647. A, binding of DCP-UO22+ to 8A11 before (a) and after (b) incubation of the antibody with Zenon 647. B, differences in the natural logarithms of the values for K0.5 obtained previously (15) for the binding of seven antigen analogs to native 8A11 minus those obtained for the binding of the same compounds to 8A11 noncovalently modified with Zenon 647. C, binding of DCP-UO22+ to the 8A11-Cy5 covalent conjugate before (a) and after (b) incubation of the 8A11-Cy5 conjugate with Zenon 647. D, differences in the natural logarithms of the values for K0.5 obtained for the binding of seven antigen analogs to 8A11-Cy5 in the absence of the Zenon 647 minus those obtained for the binding of the same compounds to 8A11-Cy5 noncovalently modified with Zenon 647.
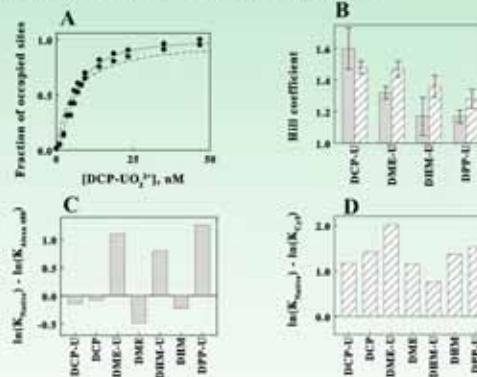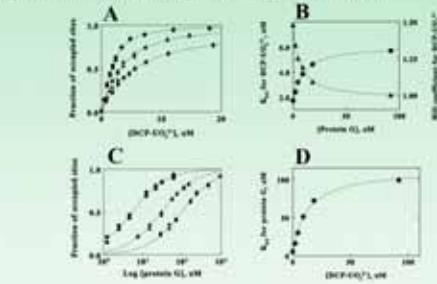

Figure 5. Heterotropic negative cooperativity in the binding of DCP-UO$_2^{2+}$ and protein G to the 8A11-Cy5 covalent conjugate. A, equilibrium binding of DCP-UO$_2^{2+}$ to 8A11-Cy5 in the presence of zero (a), 4.6 (b), and 92 (c) nM protein G. The curves drawn through the data points were generated using the Hill equation and the following respective values for K0.5 and the Hill coefficient: a, 1.7 nM and 1.48; b, 3.19 nM and 1.25; and c, 5.89 nM and 1.0. B, dependence of the values of K0.5 (circles) and the Hill coefficient (triangles) for the binding of DCP-UO$_2^{2+}$ to 8A11-Cy5 on the concentration of protein G. C, semilogarithmic plots of the equilibrium binding of protein G to 8A11-Cy5 in the presence of zero (a), 4.6 (b), and 92 (c) nM DCP-UO$_2^{2+}$. The curves drawn through the data points were generated using Eq. 1 and values for K0.5 of 5.43, 30.0, and 98.7 nM for a, b, and c, respectively. D, dependence of the value of K0.5 for the binding of protein G to 8A11-Cy5 on the concentration of DCP-UO$_2^{2+}$.
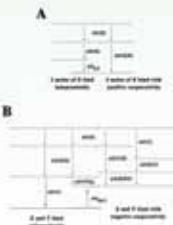

Figure 6. Schematic free energy diagrams for the binding of multiple ligands to an antibody. μ(i) represents the chemical potential of the ith species. _G(i), _G(I), and _GU represent the unconditional, the conditional, and the coupling free energy changes, respectively, of the binding reactions associated with the ith species. A, binding of two moles of antigen (X) to a divalent antibody (P). B, binding of two moles of antigen and one mole of a different ligand (Y) to spatially separate sites on an antibody.